In Situ Measurement of the Thermal Expansion Behavior of Benzocyclobutene Films

THOMAS C. HODGE, SUE ANN BIDSTRUP ALLEN, PAUL A. KOHL

School of Chemical Engineering, Georgia Institute of Technology, Atlanta, Georgia 30332-0100

Received 14 November 1997; revised 22 June 1998; accepted 26 June 1998

ABSTRACT: *In situ* measurement techniques suitable for determination of the coefficient of thermal expansion (CTE) in thin, spin-cast polymer films in both the in-plane and through-plane directions are presented. An examination of the thermal expansion behavior of cyclotene thin films has been performed. In particular, the effect of film thickness on the in-plane and through-plane CTE and in-plane Young's modulus of spin-coated cyclotene films was examined. It is shown that the mechanical response of *in situ* cyclotene films can be adequately described by isotropic film properties. It was also demonstrated that there is no thickness dependence on the free-standing mechanical properties or on the resulting through-plane thermal strain in an *in situ* film. © 1999 John Wiley & Sons, Inc. J Polym Sci B: Polym Phys 37: 311–321, 1999

Keywords: Cyclotene; modulus; polymer dielectric; stress; thermal expansion coefficient

INTRODUCTION

Electrical interconnections in microelectronic structures (e.g., integrated circuits and electronic packages) use interlayer dielectrics which separate and insulate metal conductors forming three-dimensional interconnection structures. Due to the three-dimensional nature of these structures, the thermal, electrical, and mechanical properties of the dielectric materials must be known in all directions in order to correctly design and simulate device performance. A commonly used class of polymer dielectric material, polyimides, exist in formulations which have been shown to have a high degree of orientation and exhibit anisotropic properties.[1–10] Divinyl siloxane benzocyclobutene (BCB, trade name: Cyclotene 3022, produced by Dow Chemical Co.) is a thermosetting material with low optical anisotropy. There is evidence that this low anisotropy of Cyclotene holds for mechanical and dielectric properties as well.[11,12]

It is highly desirable to understand the stresses developed between the polymer dielectrics, metal insulators, and substrates onto which they are deposited. In order to properly understand these stresses, the thermal expansion behavior of the polymer in both the in-plane and the through-plane directions must be characterized.

Measurement of through-plane mechanical properties of thin films is difficult due to the high resolution required to measure the small thickness changes for thin films. Several techniques have been applied to measure the through-plane thermal expansion of thin polymer films.[2,3,9,10,13–18] Considering the need for *in situ* measurements, three techniques are available: Fabry-Perot interferometry, two-beam laser interferometry,[3] and the parallel plate capacitor technique of Pasztor et al.[18]

The accuracy of Fabry-Perot interferometry is questionable. Tong et al. reports that the through-plane CTE of PMDA-ODA polyimide films obtained by air-gap capacitance change and thermal mechanical analysis (TMA) are approximately 85 ppm/°C.[9,10,16] The Fabry-Perot laser interferometry measurements of Tong yield a through-plane CTE of 100–130 ppm/°C for the

Correspondence to: S. A. Bidstrup Allen

Journal of Polymer Science: Part B: Polymer Physics, Vol. 37, 311–321 (1999)
 CCC 0887-6266/99/040311-11

same PMDA-ODA material.[9,10] The discrepancy between the Fabry-Perot result and that from the other techniques was attributed to errors of plate bending and tilting, not to material differences.

The two-beam laser, phase-shift technique developed by Elsner et al.[3] has yielded through-plane thermal expansion results for BPDA-PPD similar to that obtained using the air gap capacitor technique. Chen and Wagner obtained a temperature-dependent, through-plane thermal expansion of 100–200 ppm/°C for 21.7 μm thick BPDA-PPD spin-cast films on silicon.[6] This result is similar to that obtained by Wu and Questad for 75 μm free standing films using the air gap capacitor technique.[17] However, the presence of a metal overcoat over the polymer film in the two-beam interferometric technique changes the stress state of the polymer. This metal overcoat may be insignificant for a stiff polyimide such as BPDA-PPD, but may cause pronounced effects in less rigid materials. Lastly, the capacitance change technique developed by Pasztor et al.[18] is inaccurate due to the neglect of permittivity effects in the polymer dielectric.

This work uses *in situ* measurement techniques capable of accurately measuring through-plane CTE of insulating thin films. The technique is based on *in situ* dielectric measurements utilizing two electrode geometries: a comb electrode structure and a parallel-plate capacitor structure. This capacitance-based technique is similar to that of Pasztor,[18] i.e., a parallel plate capacitor is used to determine the film thickness as a function of temperature. However, the use of the comb electrode allows the permittivity changes as a function of temperature to be determined as well.

Substrate induced effects on the through-plane CTE have been modeled by Lee et al.[19] From Lee et al., it is expected that the substrate will cause an apparent increase in the through-plane CTE of the film due to Poisson's effect. For a Poisson's ratio of 0.33 (typical of Cyclotene and most polymers), the effective through-plane CTE should be twice that of the bulk material without the presence of a substrate. Thus, for Cyclotene with an isotropic CTE of 50–60 ppm/°C, in the presence of a substrate a through-plane thermal expansion of 100–120 ppm/°C is anticipated. A value higher than 100–120 ppm/°C could be attributed to either a higher Poisson's ratio or to anisotropic material properties.

This article describes *in situ* measurement techniques suitable for determination of the coefficient of thermal expansion (CTE) in thin, spin-cast polymer films, such as Cyclotene, in both the in-plane and through-plane directions. An examination of the thermal expansion behavior of Cyclotene thin films has been performed. In particular, the effect of film thickness on the in-plane and through-plane CTE and in-plane Young's modulus of spin-coated Cyclotene films was examined.

EXPERIMENTAL

In-Plane Properties

The residual stress developed between the substrate and the Cyclotene films was measured with a Flexus F2320 stress measurement system (Tencor Instruments, Sunnyvale, CA). In the Flexus system, the Stoney equation is used to determine the film stress in two dimensions:

$$\sigma = -\frac{E}{(1-v)}\frac{h^2}{6Rt} \tag{1}$$

where σ is the average film stress, $E/(1-v)$ is the biaxial modulus of the substrate (1.805×10^{11} Pa for $\langle 100 \rangle$ silicon wafers[20]), h is the substrate thickness, t is the film thickness, and R is the substrate radius of curvature. The Stoney equation for biaxially strained films shown in eq. (1) has been verified by numerous independent sources for measurement of a thin film on a thick substrate.[21–30] The radius R must be corrected for the initial curvature of the bare wafer. The uncoated wafer is scanned for the initial radius R_1, before deposition of the polymers, and then scanned again to determine R_2 after deposition of the film. Since the stress is proportional to $1/R$, it follows that:

$$\frac{1}{R} = \frac{1}{R_2} - \frac{1}{R_1} \tag{2}$$

To calculate the film CTE and biaxial modulus, the following equation is utilized[30]:

$$\frac{d\sigma}{dT} = \frac{E}{(1-v)_{\text{film}}}(\alpha_{\text{sub}} - \alpha_{film}) \tag{3}$$

where $d\sigma/dT$ is the slope of the stress versus temperature plot that is generated by the Flexus. Equation (3) has two unknowns, namely the biaxial modulus of the film, $[E/(1-v)]_{film}$, and the

CTE of the film, α_{film}. In order to solve for both unknowns, we need to perform temperature cycles with Cyclotene on at least two different substrates.

In this work, Cyclotene 3022 films were spin-cast in approximately 1, 5, and 15 micrometers thickness on three different substrates: (i) 100 mm diameter (100) silicon substrate (500 μm), (ii) 40 mm diameter gallium arsenide substrate (410 μm), and (iii) 75 mm diameter 2024-T3 aluminum substrate (650 μm). The aluminum substrate assisted in obtaining an accurate calculation of the film properties because its mechanical properties are very different from silicon and GaAs. Aluminum has a significantly higher CTE, 22.7 ppm/°C,[31] than silicon and GaAs, 3 and 6 ppm/°C, respectively.[32] Ideally, a substrate with a CTE greater than that of the Cyclotene film would be desirable to allow interpolation of the CTE of the polymer film. However, no materials with a CTE greater than 60 ppm/°C (the CTE of bulk Cyclotene) were available for this purpose; therefore, some error may be associated with the calculated CTE because of the required extrapolation of the film CTE.

Prior to film deposition, the bare substrates were temperature cycled in the Flexus F2320 to observe the radius of curvature as a function of temperature. In the case of silicon and gallium arsenide substrates, the room temperature curvature was found to be constant throughout the temperature range. For the aluminum substrate, a temperature dependence of the radius of curvature was observed and was incorporated into the calculation of the effective radius used in the stress calculation by allowing R_1 in eq. (2) to be a function of temperature. The constants used in the stress calculations (Substrate Young's modulus, Poisson's ratio, and CTE) were obtained from the CINDAS database in the case of silicon and gallium arsenide, and from the *Metal's Handbook* in the case of aluminum.[31,32]

Cyclotene film thicknesses were determined using a Metricon 2010 prism coupler system (Metricon Corporation, Pennington, NJ).[33] This system utilizes polarized laser light to nondestructively determine the index of refraction and film thickness.

Through-Plane CTE Dual Capacitor Measurement Technique

The dual capacitor measurement technique utilizes a parallel plate capacitor and a comb electrode fabricated with the same polymer dielectric. The parallel plate capacitors are dependent on the through-plane permittivity and film thickness of the dielectric film. The comb electrode structure can be used to determine the permittivity changes in dielectric films with temperature assuming isotropic dielectric properties. By combining the results from these two electrodes, the through-plane change in film thickness as a function of temperature can be determined.

An HP4263A LCR meter was used for both the parallel-plate capacitor measurements and comb electrode measurements. The measurement frequency used was 10 kHz and the measurement voltage was 1 V. 128 measurements were averaged to obtain each datum point.

The capacitance of a parallel plate capacitor is calculated using the equation

$$C = \frac{\varepsilon' \varepsilon_0 A}{t} = \frac{\varepsilon' \varepsilon_0 \pi r^2}{t} \tag{4}$$

where C is the capacitance in farads, ε' is the permittivity of the dielectric, ε_0 is the permittivity of free space (8.85×10^{-12} F/m), r is the capacitor radius in meters, and t is the dielectric thickness in meters.[34] To determine the change in capacitance with temperature, the derivative of eq. (4) with respect to temperature yields

$$\frac{dC}{dT} = \frac{d\varepsilon'}{dT}\left(\frac{\varepsilon_0 \pi r^2}{t}\right) + 2\frac{dr}{dT}\left(\frac{\varepsilon' \varepsilon_0 \pi}{t}\right) - \frac{1}{t^2}\frac{dt}{dT}(\varepsilon' \varepsilon_0 \pi r^2) \tag{5}$$

Dividing eq. (5) by eq. (4) yields

$$\frac{1}{C}\frac{dC}{dT} = \frac{1}{\varepsilon'}\frac{d\varepsilon'}{dT} + 2\frac{1}{r}\frac{dr}{dT} - \frac{1}{t}\frac{dt}{dT} \tag{6}$$

Noting that the term involving the capacitor radii is equivalent to the in-plane strain of the polymer and the final term is the through-plane thermal strain in the polymer, eq. (6) may be simplified further to

$$\frac{1}{C}\frac{dC}{dT} = \frac{1}{\varepsilon'}\frac{d\varepsilon'}{dT} + 2\alpha_{xy,in\ situ} - \alpha_{z,in\ situ} \tag{7}$$

where $\alpha_{xy,in\ situ}$ and $\alpha_{z,in\ situ}$ are the thermal strains of the polymer film as a function of temperature. The x and y directions are the in the

plane of the film and the z direction is the through-plane direction. Note that these are not the thermal expansion coefficients of the polymer in the in-plane and through-plane directions. The thermal expansion coefficients for the bulk material relate to the strains generated; however, the in-plane strain is dominated by the substrate as the thin film is assumed to be completely compliant to the expansion and contraction of the substrate. The through-plane expansion is enhanced by the presence of the substrate as discussed by Lee et al.[19] The units in eq. (7) are $°C^{-1}$ or ppm/°C, as desired. To calculate the through-plane thermal strain, $\alpha_{z,in\ situ}$, using eq. (7), the reduced capacitance change as a function of temperature is measured using parallel plate capacitors, the in-plane strain is assumed to be equal to the expansion of the substrate (for silicon, α = 2.87 ppm/°C), and the reduced permittivity change as a function of temperature is found using comb electrodes.

A theoretical derivation of the relationship between the change in permittivity with temperature and the thermal expansion of a nonpolar polymer film has been previously performed by Gevers yielding eq. (8).[35]

$$\frac{1}{\varepsilon'}\frac{d\varepsilon'}{dT} = -\alpha_{film}\left(\varepsilon' + 1 - \frac{2}{\varepsilon'}\right) \tag{8}$$

In this derivation, only isotropic density changes in the polymer are assumed to occur and dipolar orientation effects and dielectric losses are neglected. Eq. (8) has been successfully used to predict the CTE of bulk polystyrene given the dielectric constant (or permittivity in the absence of dielectric loss) as a function of temperature.[36] Eq. (8) will be compared to results from eq. (7) for spin-coated Cyclotene films. For this comparison, the film CTE in eq. (8), α_{film}, is calculated to be the average of the thermal strains in the three principle directions, i.e.,

$$\alpha_{\text{film}} = \frac{2\alpha_{\text{xy},in\ situ} + \alpha_{z,in\ situ}}{3} \tag{9}$$

Eq. (9) follows from the isotropic density changes assumed in the derivation of eq. (8). In general, eq. (8) predicts that for a nonpolar polymer with a positive coefficient of thermal expansion that the permittivity should decrease with increasing temperature due to the decrease in density of oscillators caused by the thermal expansion.

Two types of comb electrodes, interdigitated electrodes in the plane of the film, were used in this work. The first type of comb electrode was fabricated on an insulating layer (in this work, Cyclotene) which isolates the comb electrode from a metal ground plane. The testing of the sensor uses the air above the comb electrode as an internal reference and all of the changes in the capacitance of the parallel plate electrode can be attributed to the thickness changes and permittivity changes of the polymer dielectric. Actual combs have 50 fingers in each direction and a total meander length of 35 cm. The gold ground plane is 0.15 μm thick. The line widths and spacings were each 10 μm. The lift-off fabrication sequence and schematic for the comb electrode structure is given elsewhere.[11] Narrower line spacings would give higher capacitances, improving the accuracy of the measurements. However, due to fabrication considerations, wider line spacings were necessary to achieve reasonable electrode yields. Due to the position of the polymer film, the response of the comb electrode was dependent on both the thickness of the film and the permittivity of the polymer. To evaluate the comb electrode response, the parallel plate capacitance measurements must be utilized.

The second comb electrode geometry utilized is a simple pair of interdigitated combs on an inert substrate, such as glass. Sensors of this type fabricated of chromium combs on fused quartz were purchased from Micromet Instruments, Inc. (Cambridge, MA). These sensors are described in more detail by Shepard et al.[37] Unlike Micromet, the sensors used in this study have no ground plane so that all of the electric field is between the combs. The line width and spacing are 1 μm and the meander length is 1 m. The narrower line spacing and longer meander result in larger interelectrode capacitance than the gold-on-polymer structures (10 μm line/space width), described above. The larger capacitance should yield a more accurate determination of the polymer properties. These chrome-on-glass electrodes do not have a parallel-plate capacitor structure incorporated into their design. A separate wafer coated with the dielectric of interest with parallel-plate capacitors is necessary for dual capacitor testing. Errors associated with testing of films not coated on the same substrate were minimized by processing the films simultaneously.

Electrostatic modeling of the comb electrode geometry was performed using Maxwell EM simulation package (ANSOFT Co., Pittsburgh, PA). A

two-dimensional model was created consisting of two transmission lines of finite width and thickness, a supporting dielectric layer and a coating dielectric layer. The model assumed the dielectric properties of all the materials were isotropic and homogeneous.[1]

The input parameters to the electric field model are the electrode metal thickness, the distance from the center of an electrode finger to the center of the nearest space, the thickness and the dielectric properties of the insulator above and below the electrode, and the line width and spacing of the comb. Actual electrodes vary somewhat from the desired geometry due to fabrication variability, so the actual physical parameters were quantified for each electrode. To calibrate the sensor, measurement of the capacitance of the comb electrode in air was used to find the electrode geometry by interpolating simulations for a dielectric with a permittivity of one with varying line width and spacing. Line width and spacing determined from the measured electrical properties in air were used in later simulations to determine the response of the comb electrode coated with Cyclotene. In the case of the IDE on glass, the dielectric properties of the underlying dielectric changed as a function of temperature.

RESULTS

In-Plane Results

The stress as a function of temperature for 14.61 micrometer thick Cyclotene films on silicon, gallium arsenide and aluminum substrates are shown in Figure 1. The stresses are highest for the silicon substrate and lowest for the aluminum substrate, reflective of the magnitude of the CTE mismatch between the Cyclotene film and the substrate. Some curvature is seen in the stress versus temperature plot of the Cyclotene on aluminum data set. This curvature may be due to changes in the bare substrate curvature with temperature. The slopes from the stress-temperature plot are shown in Table I. Using the data in Table I in eq. (3), the calculated in-plane CTE and biaxial modulus for the 14.6 μm thick Cyclotene film are 53.8 $\pm$ 13.6 ppm/°C and 4.29 $\pm$ 1.47 GPa, respectively. The ranges are the 95% confidence intervals calculated on the linear regression. The least-squares regression provided the best fit of the two parameters for all three substrates.

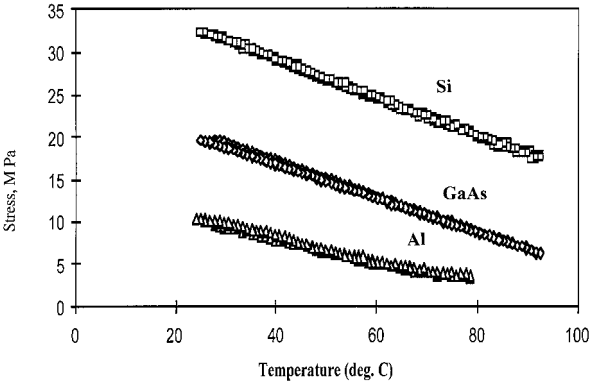

Figure 1. Stress as a function of temperature for approximately 14.6 μm thick Cyclotene.

The stress as a function of temperature for approximately 5 μm thick Cyclotene films on silicon, gallium arsenide, and aluminum substrates were measured and the slopes ($d\sigma/dT$) are shown in Table I. The measured stress changed linearly for all three substrates with very little scatter; however, the reproducibility of the room temperature stress for films on silicon was higher than for films on gallium arsenide or aluminum. The average thickness of the films is 5.33 μm. The calculated in-plane CTE and biaxial modulus for the 5.33 μm Cyclotene films from the data in Table I are 63.3 $\pm$ 13.6 ppm/°C and 2.64 $\pm$ 0.62 GPa, respectively.

Table I. Calculated Slopes and Material Properties for Cyclotene Stress-Temperature Data

Film Thickness (μm)	Slope of Stress-Temperature Plot (MPa/°C)			CTE (ppm/°C)	Biaxial Modulus (MPa)
	Silicon	GaAs	Aluminum		
1.36	−0.162 ± 0.019	−0.124	−0.101	55.8 ± 10.7	2.94 ± 1.23
5.33	−0.166	−0.145	−0.108	63.3 ± 13.6	2.64 ± 0.62
14.7	−0.204	−0.222	−0.131	53.8 ± 13.6	4.29 ± 1.47
Average				57.6 ± 12.7	3.31 ± 1.10

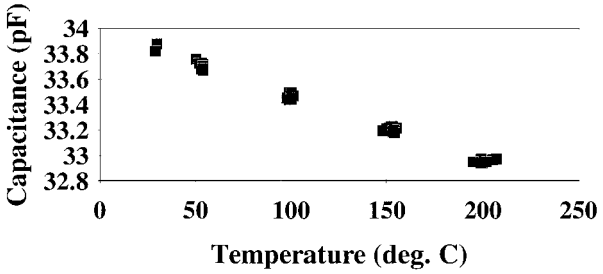

Figure 2. Capacitance as a function of temperature as determined from parallel plate capacitor measurements for a 30 μm Cyclotene film.

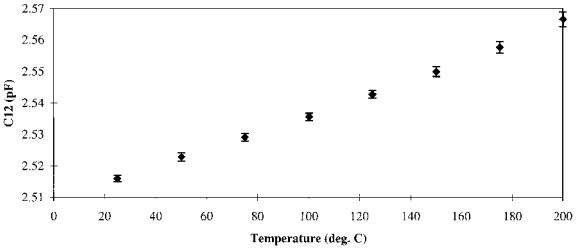

Figure 3. Interelectrode capacitance for 10 μm line/space comb electrode fabricated on 6.5 μm thick Cyclotene.

The stress as a function of temperature for approximately 1 μm thick Cyclotene on silicon, gallium arsenide, and aluminum substrates showed more scatter in the data due to the relatively small changes in the radius of curvature with temperature. A small change in the radius results in a noticeable change in the calculated stress. The slopes of the stress-temperature measurements are shown in Table I. The average Cyclotene thickness of the tested samples is 1.36 μm. Three measurements of the stress as a function of temperature on silicon were performed to examine the reproducibility of the data as well as to estimate the expected error in the calculated slopes between runs. The average slope on the silicon substrates is -0.162 MPa/°C with a standard deviation of 0.019 MPa/°C. Using the results in Table I with eq. (3), the calculated CTE and biaxial modulus for the 1.36 μm thick Cyclotene films are 55.8 $\pm$ 10.7 ppm/°C and 2.94 $\pm$ 1.23 GPa.

Through-Plane CTE Results

Parallel-Plate Capacitor Measurements

Several measurements of parallel plate capacitors with different thicknesses of Cyclotene dielectric were performed. The Cyclotene dielectric thicknesses tested were approximately 1, 6, and 30 μm thick. A typical measurement of the capacitance as a function of temperature for a parallel plate capacitor with an approximately 30 μm thick Cyclotene film is shown in Figure 2. The parallel-plate capacitance change for each thickness of film was decreased linearly as the temperature was increased. The average capacitance change as a function of temperature for each thickness is shown in Table II. The capacitance changes with temperature show no thickness dependence, indicating that the thickness and permittivity changes with temperature are similar for different thicknesses of Cyclotene. It should also be noticed that the capacitance decreases with increasing temperature as would be expected for materials where thermal expansion effects dominate.

Comb Electrode Measurements

Two types of comb electrodes were tested to extract the permittivity changes in Cyclotene as a function of temperature: one fabricated in-house with 10 μm lines/spaces and one purchased from Micromet Instruments, Inc. with 1 μm lines/spaces.

Three Cyclotene film thicknesses, 1, 6, and 30 μm, were tested using 10 μm line/space gold comb electrodes. The interelectrode capacitance of a 10 μm line/space comb electrode on 6.5 μm thick

Table II. Results from Measurements of Parallel-Plate Capacitors as a Function of Temperature

No. of Measurements	Avg. Thickness (μm)	Standard Deviation (μm)	$1/CdC/dT$ (ppm/°C)	Standard Deviation (ppm/°C)
6	1.19	0.01	-145	13
6	6.06	0.73	-148	10
3	30.7	3.8	-150	19
All (15)			-147	12

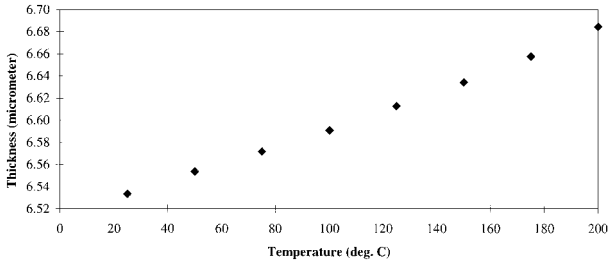

Figure 4. Film thickness as a function of temperature calculated from comb electrode in Figure 3.

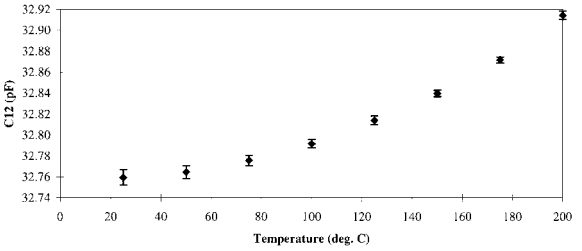

Figure 6. Interelectrode capacitance for chrome-on-glass comb electrode coated with 6.5 μm Cyclotene film. Same electrode as in Figure 5.

Cyclotene is shown in Figure 3. The electrode thickness at room temperature is 1.1 μm. Using the parallel-plate capacitor and comb electrode data at room temperature, the line width is calculated to be 11.67 μm and the spacing is 8.33 μm. The permittivity and film thickness as a function of temperature were calculated using the parallel-plate capacitor data in Table II and the comb electrode data in Figure 3. The permittivity of the Cyclotene film decreased with increasing temperature with a slope $[(1/\varepsilon')d\varepsilon'/dT)]$ of -50.9 ppm/°C. The thickness as a function of temperature obtained for the comb electrode on the Cyclotene sensor is shown in Figure 4. The thickness increased linearly as the temperature increases with a through-plane thermal strain $[(1/t)dt/dT]$ of 124.2 ppm/°C. The error associated with this comb electrode measurement is large due to the small capacitances involved.

Chrome-on-glass comb electrodes were tested with approximately 1 and 6 μm thick Cyclotene films. Due to variations in electrode fabrication, each sensor was individually characterized before and after coating. The capacitance as a function of temperature for a bare chrome-on-glass sensor and the same sensor coated with 6.5 μm Cyclotene are shown in Figures 5 and 6, respectively. Utilizing Maxwell EM simulation of the capacitance measurements at room temperature, the line width and spacing were determined. The line width and spacing were found to be 0.75 μm and 1.25 μm, respectively. The nominal line width and spacing for these electrodes is 1 μm. Utilizing the calculated line width and spacing, a correlation of the bare electrode capacitance to the substrate permittivity was determined. Using the correlation generated and the data in Figure 5, the substrate permittivity as a function of temperature was calculated, and is shown in Figure 7. The permittivity of the fused quartz substrate increases with increasing temperature. This result is typical of glass substrates which contain ionic contaminants and polar species. The 6.5 μm Cyclotene can be assumed to be semi-infinite in thickness due to the large difference between the film thickness and the electrode spacing. Using the substrate permittivity in Figure 7, the permittivity response of the Cyclotene film as a function of temperature was determined, as shown in Figure 8. The permittivity change $[(1/\varepsilon')d\varepsilon'/dT)]$ for the 6.5 μm Cyclotene film is found to be -45.6 ppm/°C. The standard deviation of this data set is 1.6 ppm/°C; however, the standard deviation between several electrodes with similar film thicknesses is 10 ppm/°C.

Using the permittivity change with the capacitance change for an approximately 6 μm thick

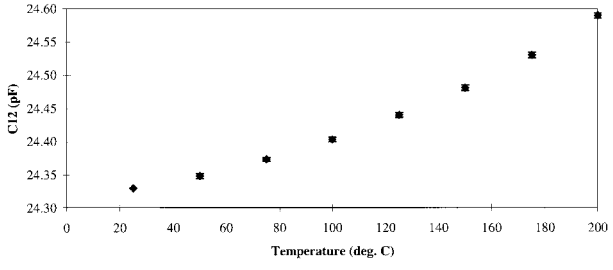

Figure 5. Interelectrode capacitance of a bare chrome-on-glass comb electrode as a function of temperature.

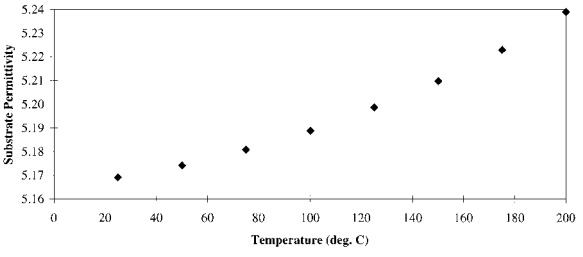

Figure 7. Permittivity of glass substrate determined from data of bare chrome-on-glass sensor in Figure 5.

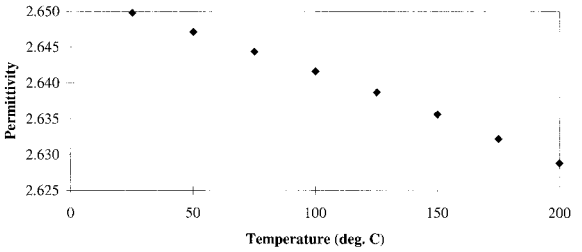

Figure 8. Permittivity as a function of temperature for 6.5 μm thick Cyclotene, determined using chrome-on-glass comb electrode.

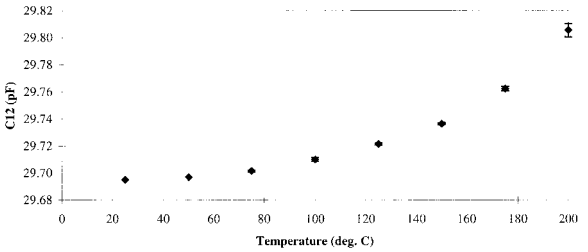

Figure 10. Interelectrode capacitance as a function of temperature for chrome-on-glass comb electrode coated with 1.2 μm thick Cyclotene. Same electrode as Figure 9.

Cyclotene film and assuming the in-plane CTE to be that of silicon (2.87 ppm/°C), the through-plane thermal strain $[(1/t)dt/dT]$ is calculated to be 107.9 ppm/°C [eq. (7)]. The variation in the through-plane thermal strain is approximately 20 ppm/°C, due to variations in the permittivity and capacitance changes. This value is comparable to the predicted through-plane thermal strain for *in situ* Cyclotene of 110–120 ppm/°C.[19]

Chrome-on-glass comb electrodes were also used to examine 1.2 μm thick Cyclotene films. The capacitance of an electrode before and after Cyclotene deposition are shown in Figures 9 and 10, respectively. By using the same method as the 6.5 μm Cyclotene film, the effective line width and spacing were calculated to be is 0.645 μm and the spacing is 1.355 μm from the room temperature capacitance of the bare and coated electrode, respectively. Utilizing this line width and spacing, a correlation of the bare electrode capacitance to the substrate permittivity was determined. Using the correlation generated and the data in Figure 9, the substrate permittivity as a function of temperature was calculated, as shown in Figure 11. The permittivity of the glass substrate increases as the temperature increases. The permittivity changes in Figures 7 and 11 are of similar magnitude and the room temperature permittivity of both electrodes are similar with a value between 5.1 and 5.2. The difference in the substrate permittivity between the samples is due to variation in the substrate material between the electrodes.

The 1.2 μm Cyclotene film cannot be assumed semi-infinite since the film thickness is about the same as the electrode spacing. For this reason, both the film thickness and permittivity changes with temperature will affect the comb electrode response. In order to relate the thickness and permittivity, the parallel plate capacitance was used as a function of temperature for the 1.2 μm thick Cyclotene film. The relative capacitance change $[(1/C)dC/dT]$ as a function of temperature used was -144.7 ppm/°C. Using the data in Figure 10 and the parallel plate capacitance at a given temperature, the film thickness and permittivity could be determined. The permittivity and film thickness as a function of temperature are shown in Figures 12 and 13, respectively. The permittivity decreased linearly as the temperature increased, with a slope $[(1/\varepsilon')d\varepsilon'/dT)$ of -31.8 ppm/°C. This permittivity response is similar to that observed for the 6.5 μm Cyclotene film considering variations between the electrodes. The thickness increased linearly with temperature with a

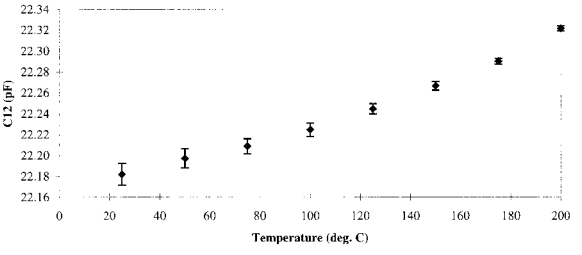

Figure 9. Interelectrode capacitance as a function of temperature for bare chrome-on-glass comb electrode.

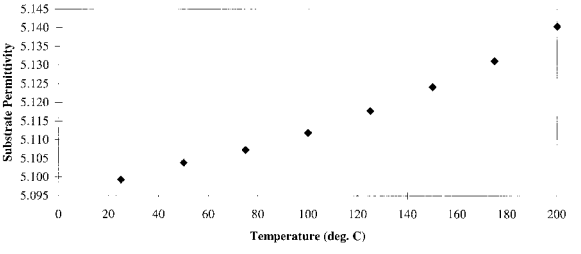

Figure 11. Permittivity of the glass substrate calculated from data in Figure 9.

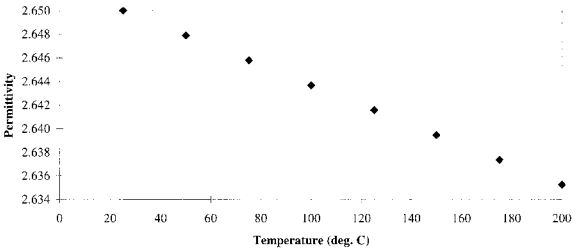

Figure 12. Permittivity as a function of temperature of 1.2 μm thick Cyclotene film calculated using data in Figure 10.

through-plane thermal strain $[(1/t)dt/dT]$ of 118.6 ppm/°C.

DISCUSSION

Cyclotene is a thermosetting benzocyclobutene polymer, known for having a very low optical anisotropy. From dielectric measurements using comb electrodes and parallel plate capacitor structures, little or no dielectric anisotropy was observed. Therefore, since Cyclotene exhibited isotropic optical and dielectric properties, isotropic mechanical properties were also expected.

The in-plane CTEs and biaxial moduli obtained for all three film thicknesses are comparable to the bulk literature values for Cyclotene of 52–60 ppm/°C and 3 GPa, respectively.[38,39] The average of the calculated in-plane CTEs is 57.6 ppm/°C which lies in the range of the literature values of CTE for Cyclotene with a standard deviation of 12.7 ppm/°C. The average biaxial modulus of the three data sets is 3.31 GPa with a standard deviation of 1.11 GPa, very close to the literature value of 3 GPa.[39] These results indicate that there is little or no thickness dependence on the in-plane mechanical properties of *in situ* Cyclotene films. It should be noted that the in-plane CTE calculated is a material property, not the actual displacement which the film undergoes. The calculation of the film stress assumes that the film expands and contracts with the substrate (no-slip condition) and that the curvature results from the stresses induced by the higher CTE film being constrained by the low CTE substrate. Therefore, in the case of a Cyclotene film on a silicon substrate, the film expands and contracts in the in-plane direction at the same rate as silicon (2.87 ppm/°C) while still having an in-plane CTE of 52–60 ppm/°C.

Using an in-plane CTE of 52–60 ppm/°C in the theoretical model for Poisson's effect discussed by Lee et al.,[19] the predicted through-plane thermal strain for an *in situ* Cyclotene film is 105–120 ppm/°C. This model assumes that the film is isotropic and that the Poisson's ratio is 0.33.

Parallel-plate capacitance measurements of Cyclotene films ranging in thickness from 1.2 μm to over 30 μm yield similar values of $[(1/C)dC/dT]$. The results of these measurements are shown in Table III. The average $[(1/C)dC/dT]$ is -147.2 ppm/°C with a standard deviation of 12.7 ppm/°C. This lack of variation with thickness indicates that the permittivity and thickness changes with temperature are not dependent on the film thickness.

Two different comb electrode geometries were used to examine the permittivity and thickness changes of spin-cast Cyclotene films. The first electrode type consists of 10 μm wide lines and spaces made of gold fabricated on top of the Cyclotene film of interest. The second electrode type has approximately 1 μm lines and spaces made of chromium on a fused quartz substrate. The capacitance of the chrome-on-glass comb electrode is approximately ten times larger than that of the gold-on-Cyclotene comb electrode. The larger capacitance allows more accurate determination of the permittivity and thickness changes in the Cyclotene films. The results of the comb electrode measurements are shown in Table III. The errors on the values in Table III are approximately 10–20 ppm/°C. The chrome-on-glass comb electrodes yield similar values of through-plane thermal strain and permittivity changes for both 1 and 6 μm Cyclotene films. The through-plane thermal strain $[(1/t)dt/dT]$ from the chrome-on-glass electrodes is between 100 and 130 ppm/°C, consistent with the predicted values. The gold-on-Cyclotene comb electrodes are inconsistent due to

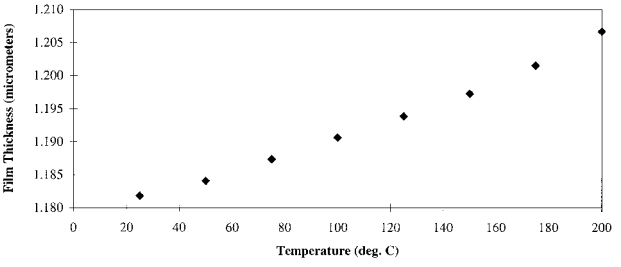

Figure 13. Cyclotene film thickness as a function of temperature determined using chrome-on-glass comb electrode and parallel-plate capacitor data.

Table III. Dual Capacitor Results for Spin-Cast Cyclotene Films

Approximate Film Thickness (μm)	Parallel-Plate Capacitor $1/CdC/dT$ (ppm/°C)	Gold-on-Cyclotene Comb Electrodes		Chrome-on-Glass Comb Electrodes	
		$1/\varepsilon' d\varepsilon'/dT$ (ppm/°C)	$1/tdt/dT$ (ppm/°C)	$1/\varepsilon' d\varepsilon'/dT$ (ppm/°C)	$1/tdt/dT$ (ppm/°C)
1	−145	139.0	290	−31.8	119
6	−148	−50.9	124	−45.6	108
30	−150	−0.5	155	—	—
Average	−147	—	—	—	—

the errors associated with the small capacitances. The 6 and 30 μm results are slightly higher than the chrome-on-glass measurements; however, the range of the thermal strains overlaps the predicted through-plane thermal strain.

The decreasing permittivity as a function of temperature for Cyclotene in Figures 8 and 12 is typical of a nonpolar dielectric. It should be noted that although a small component of Cyclotene is polar, it is mostly nonpolar. Ku and Liepins[40] observed that in a nonpolar dielectric, the permittivity is controlled by the density of the oscillators in the film. Increased distance between the oscillators decreases their electromagnetic interaction, lessening the response of the film to an alternating electric field. The positive CTE of a nonpolar film causes a net decrease in the density of oscillators in the film as the temperature increases, thus reducing the film permittivity. The results for Cyclotene do not allow prediction of the permittivity of other dielectric polymers, such as polyimide due to their higher polarity which contribute to the film permittivity. These polar groups have increased mobility as the polymer density decreases leading to an increase in their polarizability. The permittivity of a polar film can decrease, increase, or remain constant depending on the relative magnitude of the increase in the polarizability of the polar species and the decrease in the density of the oscillators.[35] A polymer with a small number of polar substituents or weak polarizability may be dominated by the nonpolar density effects yielding a decreasing permittivity with temperature. A highly polar polymer would have an increasing permittivity due to the domination of the rising polarizability with increasing temperature.

The chrome-on-glass comb electrodes [$(1\varepsilon')\mathring{d}\varepsilon' dT$] indicate that the permittivity of Cyclotene decreases with increasing temperature at a rate of −30 to −50 ppm/°C. The decrease in permittivity is consistent with expected changes in nonpolar materials.[40] Eq. (8) has previously been used to predict the permittivity change of polystyrene films. The volumetric thermal strain from eq. (9) is 40.3 ppm/°C, assuming in-plane strain equal to silicon (2.87 ppm/°C) and a through-plane thermal strain of 115 ppm/°C. Assuming a film permittivity of 2.65, the relative permittivity change predicted by eq. (8) is −116.5 ppm/°C. This result is 2 to 3 times larger than the actual permittivity change measured in this work. The discrepancy between the measurement and the prediction from eq. (8) may be due to violation of an assumption used to derive eq. (8). If significant dipolar effects exist in a polymer, the permittivity would increase as the density increases. If Cyclotene has a combination of nonpolar effects and dipolar effects, the combination could yield a more moderate change in permittivity as a function of temperature than predicted by a pure nonpolar material.

Results from this work indicate that the mechanical response of *in situ* Cyclotene films can be adequately described by isotropic film properties. This work also demonstrates that there is no thickness dependence on the free-standing mechanical properties or on the resulting through-plane thermal strain in an *in situ* film. A measurement technique based on dielectric measurements has been demonstrated for measurement of through-plane thermal expansion of *in situ* polymer films. Chrome-on-glass comb electrodes with 1 μm lines and spaces have been demonstrated to be adequate to measure permittivity and thickness changes of films 1 μm and greater.

The financial support of the National Science Foundation through the Georgia Tech Engineering Research Center. The donation of Cyclotene from Dow Chemical are gratefully acknowledged.

REFERENCES AND NOTES

1. Lin, L.; Bidstrup, S. A. J Appl Polym Sci 1993, 49, 1277–1289.
2. Pottiger, M. T.; Coburn, J. C. Polymers for Microelectronics, ACS Symposium Series, American Chemical Society, Washington, DC, 1992.
3. Elsner, G.; Kempf, J.; Bartha, J. W.; Wagner, H. H. Thin Solid Films 1990, 185(1), 189–197.
4. Herminghaus, S.; Boese, D.; Yoon, D. Y.; Smith, B. A. Appl Phys Letters 1991, 59(9), 1043–1045.
5. Boese, D.; Herminghaus, S.; Yoon, D. Y.; Swalen, J. D.; Rabolt, J. F. MRS Symp Proc 1991, 227, 379–386.
6. Chen, S. T.; Wagner, H. H. J Electron Mater 1993, 22(7), 797–799.
7. Russell, T. P.; Gugger, H.; Swalen, J. D. J Polym Sci Polym Phys Ed 1983, 21, 1745–1756.
8. Takahashi, N.; Yoon, D. Y.; Parrish, W. Macromolecules 1984, 17, 2583–2588.
9. Tong, H. M.; Hsuen, H. K. D.; Saenger, K. L.; Su, G. W. Rev Sci Instrum 1991, 62(2), 422–430.
10. Tong, H. M.; Saenger, K. L.; Su, G. W. ANTEC Proc 1991 1991, 1727–1730.
11. Hodge, T. C. Ph.D. thesis, Georgia Institute of Technology, 1996.
12. Weinberg, S. A. In-Plane Permittivity of Spin-Coated Polymer Films, M.S. thesis, Georgia Institute of Technology, 1996.
13. Elsner, G.; Kempf, J.; Bartha, J. W.; Wagner, H. H. Thin Solid Films 1990, 185(1), 189–197.
14. Chen, S. T.; Wagner, H. H. J Electron Mater 1993, 22(7), 797–799.
15. Pietila, D.; DeBra, L.; Guan, J.; Lee, C. MRS Symp Proc 1991, 203, 289–294.
16. Saraf, R. F.; Tong, H. M.; Poon, T. W.; Silverman, B. D.; Ho, P. S.; Rossi, A. R. J Appl Polym Sci 1992, 46, 1329–1337.
17. Wu, T. Y.; Questad, D. L. MRS Symp Proc 1992, 264, 143–160.
18. Pasztor, A. J.; Radler, M. J.; Curphy, J. J.; Martinez, S. J.; Langhorst, M. A. "Determination of the Linear Coefficient of Thermal Expansion in the Thickness Direction for Thin Films," Presented at ACS Meeting, March 1994.
19. Lee, J. B.; Allen, M.; Hodge, T. C.; Bidstrup-Allen, S. A.; Kohl, P. A. J Appl Polym Sci: Part B, Polym Phys 1996, 34, 1591–1596.
20. Brantley, W. A. J Appl Phys 1973, 44, 534.
21. Brenner, A.; Senderoff, S. J Res National Bureau of Standards 1949, 42, 105–133.
22. Pan, J. T.; Blech, I. J Appl Phys 1984, 55(8), 2874–2880.
23. Olsen, G. H.; Ettenberg, M. J Appl Phys 1977, 48, 2543.
24. Jaccodine, R. J.; Schlegel, W. A. J Appl Phys 1966, 37, 2429.
25. Bauer, C. L.; Farris, R. J. Polyimides: Materials, Chemistry and Characterization, Elsevier Science Publishers B. V., Amsterdam, 1989.
26. Sinha, A. K.; Levinstein, H. J.; Smith, T. E. J Appl Phys 1978, 49(4), 2423.
27. Tessier, T. G.; Adema, G. M.; Turlik, I. Proc Elec Component Conf, IEEE 1989, 127.
28. Jou, J.-H.; Huang, P.-T. Macromolecules 1991, 24, 3796.
29. Elsner, G. J Appl Polym Sci 1987, 34, 815.
30. Merriman, B. T.; Craig, J. D.; Nader, A. E.; Goff, D. L.; Pottiger, M. T.; Lautenberger, W. J. Proc Elec Component Conf, IEEE 1989, 155.
31. Metals Handbook Ninth Edition, vol. 2 Properties and Selection: Nonferrous Alloys and Pure Metals, American Society for Metals 1979, 72–78.
32. Center for Information and Numerical Data Analysis and Synthesis (CINDAS) Microelectronic Material Database, Purdue University.
33. Adams, A. C.; Schinke, D. P.; Capio, C. D. J Electrochem Soc: Solid State Sci Technol 1979, 126, 1539–1543.
34. ASTM D150-92, Standard Test Methods for A-C Loss Characteristics and Permittivity (Dielectric Constant) of Solid Electrical Insulating Materials, 1992.
35. Gevers, M. Philips Res Rep, 1946, 1, 197–224.
36. Aldrich, P. Encyclopedia of Polymer Science & Engineering, 2nd Ed., 16, John Wiley & Sons, New York, 1989; pp 161–165.
37. Shepard, N. F.; Day, D. R.; Lee, H. L.; Senturia, S. D. Sensors and Actuators 1982, 2, 263–274.
38. Burdeaux, D.; Townsend, P.; Carr, J.; Garrou, P. E. J Electron Mater 1990, 19, 1357.
39. Garrou, P. E. et al., in Proc ECTC, 1992; also IEEE Trans Components, Hybrids, Manuf Technol, 1992, 770.
40. Ku, C. C.; Liepins, R. Electrical Properties of Polymers: Chemical Principles, Hanser Publishers, New York, 1987; pp 54–55.